Published in final edited form as:
Cancer Res. 2009 February 15; 69(4): 1668–1677. doi:10.1158/0008-5472.CAN-07-6385.

STATs MEDIATE FIBROBLAST GROWTH FACTOR INDUCED VASCULAR ENDOTHELIAL MORPHOGENESIS

Xinhai Yang, **Dianhua Qiao**, **Kristy Meyer**, and **Andreas Friedl**
Department of Pathology and Laboratory Medicine, University of Wisconsin-Madison, WI 53792

Abstract

The fibroblast growth factors (FGFs) play diverse roles in development, wound healing and angiogenesis. The intracellular signal transduction pathways which mediate these pleiotropic activities remain incompletely understood. We show here that the proangiogenic factors FGF2 and FGF8b can activate signal transducers and activators of transcription (STATs) in mouse microvascular endothelial cells. Both FGF2 and FGF8b activate STAT5 and to a lesser extent STAT1, but not STAT3. The FGF2-dependent activation of endothelial STAT5 was confirmed *in vivo* with the matrigel plug angiogenesis assay. In tissue samples of human gliomas, a tumor type where FGF-induced angiogenesis is important, STAT5 is detected in tumor vessel endothelial cell nuclei, consistent with STAT5 activation. By forced expression of constitutively active or dominant-negative mutant STAT5A in mouse brain endothelial cells, we further show that STAT5 activation is both necessary and sufficient for FGF-induced cell migration, invasion and tube formation, which are key events in vascular endothelial morphogenesis and angiogenesis. In contrast, STAT5 is not required for brain endothelial cell mitogenesis. The cytoplasmic tyrosine kinases Src and Janus kinase 2 (Jak2) both appear to be involved in the activation of STAT5, as their inhibition reduces FGF2 and FGF8b induced STAT5 phosphorylation and endothelial cell tube formation. Constitutively active STAT5A partially restores tube formation in the presence of Src or Jak2 inhibitors. These observations demonstrate that FGFs utilize distinct signaling pathways to induce angiogenic phenotypes. Together, our findings implicate the FGF-Jak2/Src-STAT5 cascade as a critical angiogenic FGF signaling pathway.

Keywords

FGF; STAT; Src; Jak2; angiogenesis; endothelial cells

Introduction

Malignant neoplasms depend on the induction of new blood vessels (angiogenesis) for continued growth and metastatic spread (1,2). Angiogenesis combined with aberrant endothelial cell (EC) proliferation is particularly evident in high-grade gliomas (3). Because of the apparent reliance of gliomas on angiogenesis and the lack of effective treatments, angiogenesis inhibition is a promising therapeutic approach in this highly lethal tumor type. The rational design of such treatment strategies, however, requires a more complete understanding of the biology of angiogenesis regulation.

Many members of the fibroblast growth factor (FGF) family rank among the most potent angiogenic stimulators (4). FGFs signal via four known receptor tyrosine kinases (FGFR1-4).

Address correspondence to: Andreas Friedl, University of Wisconsin-Madison, Department of Pathology and Laboratory Medicine, Clinical Sciences Center K4/812, 600 Highland Avenue, Madison, WI 53792, E-mail: afriedl@wisc.edu.

Ligand specificity is provided by alternative splicing events affecting the FGFR extracellular domain and by heparan sulfate proteoglycan co-receptors (5,6). The present study focuses on FGF2 and FGF8b, two growth factors with well documented roles in tumor angiogenesis, which signal via different FGFRs (7,8). FGF2 is thought to signal primarily through FGFR1c whereas FGF8b signals via FGFR3 and 4 (6). Ligation of the FGFR leads to receptor transphosphorylation and the activation of several parallel signaling pathways (9–11). In one such pathway, a docking complex, which includes FRS2 and Grb2, stimulates the classical ras-raf-MEK-MAPK signaling cascade (11). An alternative pathway involves Gab1, PI3K and Akt (12). MAPK-mediated signaling is thought to control mitogenesis, whereas Akt has been implicated primarily in cell survival regulation. It is unlikely, however, that these two pathways mediate all of the pleiotropic FGF effects.

The signal transducers and activators of transcription (STATs) are best characterized as downstream mediators of cytokine signaling (13). Recent evidence has implicated these transcription factors in FGF-triggered pathways although their relative contribution has not been fully explored (14). STAT1 is specifically activated in chondrocytes of thanatophoric dysplasia patients, which carry a constitutively active mutant of FGFR3 (15). In human umbilical vein ECs, STAT3 is phosphorylated in response to FGF2 (16). Interestingly, phosphorylated STAT3 has been detected in activated ECs of high-grade gliomas, suggesting a role for STATs in angiogenesis of this tumor type (17). This raises questions about signaling intermediaries between the FGFRs and STATs. Src kinases can activate STATs and are established players in FGF signaling (18–21). Janus kinase 2 (Jak2) is typically implicated as an upstream activator of STATs (22), although little evidence links this enzyme to the FGFR-STAT axis.

Angiogenesis requires the orchestration of a sequence of events, which include migration and invasion of ECs into the stroma surrounding the pre-existing vessel, proliferation along the migration path and differentiation into a new vessel tube. FGFs are capable of stimulating all of these processes but there is very little information on the physiologic role of the different intracellular signaling pathways in regulating these cellular responses. The purpose of this study was to examine the function of STAT signaling downstream of the FGFR in EC responses. We describe a novel role for the Jak2/Src-STAT5 cascade in mediating FGF-induced migration, invasion and tube formation of brain ECs.

Materials and Methods

Cell culture

Tissue-specific, conditionally immortalized microvascular EC lines from H-2Kb-tsA58 mice [gifts from Isaiah J. Fidler (23)], which have previously been extensively characterized and shown to retain their EC characteristics, were maintained in DMEM supplemented with 10% FBS at 33°C. The cells were cultured at 37°C for 24 hr to abolish the SV40 large T antigen before the experiments. Mouse brain microvascular ECs (BMVECs) were used for all experiments unless stated otherwise.

Antibodies and reagents

Stock solutions (10.0 μM) of recombinant human FGF2 (Pepro Tech, www.peprotech.com) and recombinant mouse FGF8b (gift from Alan C. Rapraeger, University of Wisconsin) were diluted in DMEM containing 0.2% BSA to their final concentration and added to cultures for different time periods. All monoclonal antibodies and antisera were obtained from commercial sources. Antibodies to the following antigens were obtained from Santa Cruz Biotechnology (www.scbt.com): STAT5 (C-17), STAT3 (H-190); p-STAT3 (B-7); STAT1αp91 (M-23), p-STAT1 (A-2), and Jak2 (C-20 for immunoprecipitation and HR-785 for immunoblots).

Antibodies to p-STAT5A/B (8-5-2) and p-Jak2 (Tyr1007/1008) were from Upstate Biotechnology (www.upstate.com). Antibodies against Flag (F-3165) and β-actin (AC-74) were from Sigma (www.sigmaaldrich.com). Antibodies to p-Src family (416), p-44/42 and Erk1/2 were from Cell Signaling Technology (www.cellsignal.com). Monoclonal anti-BrdU antibody (clone Bu20a) was purchased from Dako (www.dakousa.com). The kinase inhibitors PP2/PP3 and AG490/AG9 were from Calbiochem (www.emdbiosciences.com). Collagen Type I and Matrigel invasion chambers were purchased from BD Biosciences (www.bdbiosciences.com).

Adenoviral plasmids

A constitutively active STAT5A mutant (STAT5A-CA) harboring a COOH-terminus Flag tag (pRKmSTAT5AHSFlag; generated from pRKmSTAT5AcFlag using site-directed mutagenesis by substituting His299 and Ser711 with arginine and phenylalanine, respectively) and a dominant-negative STAT5A mutant (STAT5A-DN) truncated from amino acid 713 to 793 (pRKmSTAT5A713Flag) were obtained from Steven J. Collins [Fred Hutchinson Cancer Center, Seattle, 6 WA; (24,25)]. Both mutant forms of STAT5A with Flag tags were removed from the *Eco*RI and *Eco*RV sites and then inserted into the *Eco*RI and *XBa*I sites of pDNR-1r to give pDNR-1r-mSTAT5AHSFlag and pDNR-1r-mSTAT5A713Flag. Then both donor vectors were reacted with Cre BD Adeno-X LP vector using the BD Adeno-XTM Expression System 2 to produce recombinant Adeno-X-viral DNAs.

Gene transfer mediated by adenovirus

For adenovirus generation, linearized recombinant Adeno-X plasmids were transfected into 293 cells with FuGene6 (Roche, www.roche-applied-science.com). When a cytopathic effect emerged, cells were collected and frozen and thawed 3 times in sterile PBS. To produce the viral stock, the adenovirus was amplified through an additional round of 293 cell infection. Characterization and titration of the viruses were carried out by infecting 293 cells with serially diluted viral stock, counting plaque-forming units (PFUs), and Western blotting with anti-Flag antibody. For infection of target cells, brain ECs (5×10^5 cells/well) were seeded into 10 cm dishes one day prior to infection. A fixed volume of a viral stock (25 pfu) was used to infect the target cells for 24 hr. The infected brain ECs were then starved in 0.2% BSA DMEM medium for 24 hr and treated with FGFs for the subsequent experiments.

Assessment of cell growth

DMEM supplemented with 0.2% BSA or different concentrations of FBS was added to each well of a 24-well plate and cells were pretreated with or without growth factor. After 96 hr of incubation, the cells were washed with ice-cold saline, trypsinized, stained with Trypan Blue and counted. DNA synthesis was measured with a chemiluminescence-based bromodeoxyuridine (BrdU) ELISA according to Hawker with modifications (26). Cells were starved (0.2% BSA DMEM, 24 hrs) and subsequently stimulated with FGFs (24 hr with indicated concentrations of FGF2 or FGF8b in starvation buffer). BrdU (10 μM final concentration; Sigma) was added for the last 6 hrs. At the conclusion of labeling, cultures were fixed with 70% EtOH (20 min, RT), acid denatured with 2 M HCl (20 minutes, 37°C), neutralized with 0.1 M borate buffer (pH 9.0, 5 minutes, RT) and treated with blocking buffer (2% goat serum in PBS with 0.1% Triton X-100). Primary monoclonal anti-BrdU antibody was used at 1 μg/ml (60 min, 37°C; Dako, clone Bu20a). After washing to remove unbound antibody, the cells were incubated with horseradish peroxidase (HRP) conjugated secondary antibody followed by chromogenic detection in a plate reader.

Immunoblot

Cells (P100mm dishes) were washed 3 times with cold PBS and lysed with 150 ml of RIPA buffer supplemented with protease and phosphatase inhibitors on ice for 20 minutes. Cell lysates were collected by scraping, followed by centrifugation at 13,000 rpm for 20 minutes at 4°C. Protein concentration was measured by BCA assay and the lysates were mixed with 5x sample buffer. After boiling for 5 minutes, 50 mg of total protein from each sample were separated on a 7.5–12% SDS-PAGE gel. After transfer, the nitrocellulose membranes were blocked and incubated with antibodies against the phosphorylated proteins in Tris-buffered saline containing 5% nonfat dry milk plus 0.5% Tween 20, overnight at 4°C. After washing and incubating with a HRP-conjugated secondary antibody, the phosphorylated proteins were revealed using a enhanced chemiluminescent detection kit (Pierce). Membranes were then stripped and reprobed with antibodies against the non-phosphorylated proteins and developed as described above.

Immunoprecipitation

Cells (P100mm dishes) were lysed in 1 ml of ice-cold lysis buffer. Cell lysates were collected by scraping and cleared at 13,000rpm for 20 minutes at 4°C. Protein concentrations were determined by BCA assay and 1000 μg of cellular proteins were immunoprecipitated with pre-conjugated anti-STAT5A-PAA beads for 6–12 hrs at 4°C. Antibody complexes were washed 3 times with lysis buffer, then mixed with 2x sample buffer and boiled for 10 minutes. Then 40 μl of the samples were loaded to assay for p-STAT5 and STAT5.

Preparation of nuclear fractions

After treatment, the cells were washed twice with ice-cold PBS and scraped into fresh PBS. The cells were washed rapidly once with hypotonic buffer (10 mM HEPES, pH 7.9; 1.5 mM $MgCl_2$; 10mM KCl; 0.2mM PMSF; 0.5mM DTT) and the supernatant discarded. Cell pellets were then resuspended in 500 μl fresh hypotonic buffer and allowed to swell for 30 min on ice. After homogenization in a Dounce homogenizer, nuclei were collected by centrifugation for 15 minutes at 3300 g. The nuclear preparation was washed once gently with fresh hypotonic buffer. The nuclei were then lysed and analyzed for p-STAT1, -3 and -5 as described for immunoblots.

Immunofluorescent detection of p-STATs and p-Src in brain ECs

Brain ECs were cultured in 8-well chamber slides for 24 hrs to a confluency of 40–50%. After rinsing with PBS, 100 μl starvation medium was added for 24 hrs. The medium was replaced with 100 μl fresh starvation medium supplemented with FGF2 or FGF8b at 10 nM and incubated for different lengths of time. Then the cells were rinsed with cold PBS and fixed in 4% paraformaldehyde. After blocking, primary and fluorescence-labeled secondary antibodies were used at a 1:100 dilution and incubated at 37°C for 1 hr in a humidified chamber. The slides were then mounted and examined by fluorescence microscopy.

Collagen gel EC tube formation assay

Collagen gels were prepared according to a previous report (27). Briefly, a 12-well tissue culture plate was pre-chilled at −20°C and carefully coated with growth factor-reduced collagen (1.3 μg/ml; 500 μl/well; BD Biosciences, MA). The plate was incubated at 37°C for 1 hr to allow the collagen to solidify. Brain ECs (15,000 cells/well) were seeded on the surface of the collagen gel in starvation medium with or without FGF2 or FGF8b (10 nM). After 12–24 hrs, images of the tube structure were captured under phase contrast microscopy using a SPOT RT Slider digital camera (Diagnostic Instruments, www.diaginc.com) and analyzed using *ImageJ* (http://rsb.info.nih.gov/ij/). Tube length was assessed by drawing a line along each

tubule and measuring the length of the line in pixels. Tube length was measured for each sample in five non-overlapping fields under 200x original magnification.

Monolayer wound healing assay

Brain ECs were seeded onto 6-well plates at 5×10^5 cells/well and grown to confluence prior to a 24 hrs starvation period in DMEM with 0.2% BSA. A single scratch wound was introduced in the monolayer using a micropipette tip, and the medium was replaced with DMEM supplemented with FGF2 or FGF8b at 10 nM. Wound closure was monitored for 48 hrs.

Invasion assay

EC invasion was assayed using modified invasion chambers with polycarbonate PVP-free Nucleopore filters (8 μm pore size), coated with 25 μg/filter Matrigel (BD Bioscience). Brain ECs (2×10^5 cells/well) infected with Ad-Con, Ad-STAT5A-CA or Ad-STAT5A-DN and suspended in DMEM containing 0.2% BSA were added to the upper chamber in the absence of FGFs. Medium containing FGFs (10 nM) was placed in the lower chamber as a chemoattractant. At the end of a 48-hr incubation period, the cells on the upper surface of the filter were removed with a cotton swab and cells on the lower surface of the filter were stained with Hoechst 33342 (1 μg/ml) and counted. Each assay was performed in triplicate.

Matrigel plug in vivo angiogenesis assay

Growth factor-reduced matrigel (BD Biosciences) was adjusted to a concentration of 6.5 mg/ml with DMEM and mixed with FGF2 or FGF8b (20 ng/ml) and heparin (0.0025 units/ml). Matrigel for the control group was supplemented with heparin, only. The matrigel preparations (0.7 ml) were injected subcutaneously into the flanks of 4–6 week old BALB/C mice (n=6/group) with a 21 G needle and permitted to solidify. After 7 days, the mice were euthanized and the matrigel plugs were completely excised with the surrounding tissue. The samples were fixed in 10% neutral buffered formalin, embedded in paraffin and sectioned for immunohistochemistry. After epitope retrieval and blocking, paraffin sections of the matrigel plugs were labeled with antibodies to STAT5A (1:200; ST5a-2H2, Zymed), p-STAT5 (1:50; Upstate) and CD31 (1:100, Pharmingen) followed by chromogenic detection. The labeling reactions were carried out on a Labvision automated instrument. ECs invading into the gels were identified by CD31 positivity. Nuclear STAT5A was scored by evaluating both the percentage of positive ECs (>0–1%=1, 1–5%=2, >5%=3) and labeling intensity (negative=0; weak=1; moderate=2; strong=3) and multiplying the values for each sample.

Immunohistochemistry on archival human tissues

Sections from two tissue microarrays containing de-identified human glioma tissues and non-neoplastic brain controls (28) were exposed to heat-induced epitope retrieval for 90 minutes. The anti-STAT5A antibody (ST5a-2H2, Zymed) was applied at a dilution of 1:250 at room temperature for 2 hours. Bound antibody was visualized with the Ventana detection system including signal amplification using an automated immunostainer according to the manufacturer's protocol (Ventana,Medical, www.ventanamed.com). Only intense nuclear staining was considered positive.

Results

FGF2 and FGF8b stimulate brain EC proliferation

Among the 23 FGF family members, FGF2 and FGF8b have well documented pro-angiogenic acivities and are thought to signal via different FGFRs (6–8). Because mitogenesis is an important component of the angiogenic cascade, we determined the proliferative response of mouse microvascular ECs to FGF2 and FGF8b. ECs from different organ sites were included

to detect a potential heterogeneity in response. Both FGFs are similarly effective in stimulating the proliferation of ECs from brain, bone, lung and prostate, demonstrating that mitogenesis is a universal response of different ECs to FGF2 and FGF8b. (Fig. 1). Maximal DNA synthesis stimulation was achieved at a growth factor concentration of 10 nM. Therefore, this concentration was chosen for subsequent experiments.

FGF2 and FGF8b activate STATs in brain ECs

Recently, STAT transcription factors have been shown to take part in FGF signaling with a potential impact on angiogenesis regulation (16). This prompted us to examine the role of STATs in FGF signaling in BMVECs. These experiments focused on STAT1, STAT3 and STAT5, based on prior work by other investigators with other cell types (14,15,29). Both FGF2 and FGF8b activate STAT5 and to a lesser extent STAT1 in a time-dependent fashion, whereas STAT3 phosphorylation remains unchanged (Fig. 2A). FGF2-induced STAT5 activation peaks at 10 minutes, whereas FGF8b-induced STAT5 activation reaches maximum stimulation at approximately 20 min. In microvascular ECs from bone, FGF2 and FGF8b trigger a robust, transient phosphorylation of STAT3, which peaks at approximately 20 minutes and declines at 40 minutes (Fig. S1). FGF2 also activates STAT5 in a time-dependent manner for at least 40 minutes but in contrast, no STAT1 activation is detected. This suggests that different STAT family members are activated in endothelial cells in different organ sites. Because members of the MAPK family (e.g. ERK1/2) and Src proteins have been shown to play critical roles in mediating FGF-induced EC proliferation, ERK1/2 and Src activation were also examined (20). As expected, both FGF2 and FGF8b effectively activate ERK1/2 and Src in BMVECs under the same conditions used for STAT analysis (Fig. 2C, D).

FGF2 and FGF8b treatments result in nuclear translocation of phosphorylated STAT1 and STAT5

Tyrosine phosphorylation is necessary but not sufficient for STAT activation. STATs have to translocate to the nucleus in order to function as transcription factors (30). Therefore, we examined the presence of phosphorylated (p-) STAT1, STAT3, and STAT5 in nuclear extracts in response to FGF treatment. The results were overall congruent with the immunoprecipitation data as p-STAT5 and p-STAT1 translocate to the nucleus upon FGF2 or FGF8b stimulation of brain ECs, whereas neither FGF2 nor FGF8b increases nuclear p-STAT3 (Fig. 3A).

To further confirm the nuclear translocation of phosphorylated STAT1, -3, and -5, we examined the localization of STAT proteins in brain ECs by immunocytochemistry. In accordance with the biochemical data, both STAT1 and STAT5 proteins translocate to the nucleus upon FGF2 or FGF8 stimulation. STAT1 and -5 begin to accumulate in the nuclear compartment 5 minutes after the addition of FGF2 and FGF8b. From 10 to 20 minutes onward, phosphorylated STAT1 and -5 are predominantly detected within the nuclei. In contrast, phosphorylated STAT3 does not shift into the nuclear compartment upon FGF2 or FGF8b stimulation (Fig. 3B). In summary, FGF2 and FGF8b induce the nuclear translocation of STAT proteins, further implicating STAT activation in FGF signaling.

STAT5 is activated during angiogenesis in vivo

Because of the robust, FGF-dependent stimulation of STAT5 in both EC types, we decided to examine STAT5 activation during angiogenesis *in vivo*, using the subcutaneous matrigel plug assay. Compared to the control plugs, which showed some EC invasion but only minimal vessel formation, FGF2-containing matrigel was characterized by intense EC invasion and vessel formation. The FGF8b-containing plugs were indistinguishable from the control plugs. Since the pro-angiogenic effect of FGF2 in this assay is amply documented (31), we did not further quantify blood vessel density in the gels. ECs in all three groups contained cytoplasmic STAT5A (Fig. 3C). Semiquantitative analysis of nuclear STAT5A in ECs revealed

significantly elevated labeling scores in FGF2-containing gels (3.0±1.3 SD) compared to controls (0.17±0.4SD; $P < 0.01$). FGF8b treatment did not increase nuclear STAT5A, indicating that this FGF family member does not induce detectable STAT5 activation in subcutaneous ECs in this model. In the FGF2-containing gels but not the controls or FGF8b gels, focal nuclear p-STAT5 was observed (Fig. 3C).

Since FGFs, particularly FGF2, play a role in glioma angiogenesis, one would predict STAT5A activation in glioma vessel endothelial cells *in vivo*. We analyzed human tissue microarrays containing 56 gliomas (49 astrocytomas and 7 oligodendrogliomas) and 36 non-neoplastic gliosis lesions. Among the 56 glioma tissue cores, 35 contained interpretable blood vessels. Strong nuclear labeling of vascular ECs with an antibody to STAT5A was seen in 10 of these 35 tumors, contrasting with 2 out of 36 nonneoplastic tissues (P=0.012) (Fig. 3D). We were unable to detect any labeling with the phospho-specific STAT5 antibody in the small tumor samples present in the array slides.

STAT5 is not involved in FGF2- and FGF8b-induced mitogenesis

Since FGF2 and FGF8b are potent stimulators of EC proliferation (Fig. 1) and activate the STAT5 transcription factor (Fig. 2, Fig 3), we explored whether STAT5 is involved in mitogenesis regulation. To determine whether STAT5 activation is necessary and/or sufficient for EC mitogenesis induction, a constitutively active STAT5A mutant harboring a COOH-terminus Flag tag (STAT5A-CA) or a dominant-negative STAT5A truncated at amino acid 713 (STAT5A-DN) were introduced into BMVECs by adenoviral transduction (24,25,32). As monitored by adenovirally delivered green fluorescent protein (GFP), infection efficiency was greater than 95% (data not shown). Western blots confirm that the STAT5A constructs are efficiently expressed in the infected cell populations (Fig. 4A). Immunofluorescence staining revealed that STAT5A-CA is distributed throughout the cytoplasm. Only nuclear localization is detected with the phosphospecific antibody. In contrast, STAT5A-DN is not found in the nucleus and blocks the nuclear translocation of endogenous STAT5A in response to FGF (Fig. 4B). The forced expression of STAT5A-CA or STAT5A-DN had no significant effect on cell number or DNA synthesis (Fig. 4C, D). These results indicate that FGF2- or FGF8b-induced mitogenesis in brain ECs is independent of STAT5 activation.

STAT5 is required for EC migration, invasion and tube formation

To investigate further the role of FGF-dependent STAT5 activation in the regulation of angiogenic events, we analyzed EC migration, invasion and tube formation as *in vitro* angiogenesis surrogates. BMVECs were infected with control virus, STAT5A-CA or STAT5A-DN. Cell migration was determined by a monolayer wounding assay in the presence or absence of FGF2 or FGF8b. Cells expressing STAT5A-CA exhibit enhanced migration compared to control cells whereas diminished migration is seen in cells expressing STAT5A-DN (Fig. 5A, upper panels). Both FGF2 and FGF8b stimulate migration in control virus infected cells. STAT5A-CA stimulate migration to the level seen in FGF2- and FGF8b-treated cells (Fig. 5A, bar graph). Conversely, STAT5A-DN abolish FGF2- and FGF8b-induced migration, indicating that this migration requires STAT5 activation. Similarly, STAT5A-CA expression is sufficient to induce invasion through matrigel-coated membranes in the absence of FGF2 or FGF8b, whereas STAT5A-DN suppresses FGF2 and FGF8b-induced invasion (Fig. 5B).

EC tube formation in collagen gels is considered one of the most relevant in vitro angiogenesis assays (33). As expected, FGF2 and to a lesser degree FGF8b induce tube formation (Fig. 5 C). STAT5A-CA exhibits an activity similar to FGF2, suggesting that STAT5 activation is sufficient for tube formation. Importantly, expression of STAT5A-DN abolishes FGF2- and FGF8b-stimulated activity, demonstrating that STAT5 activation is required for FGF-induced

tube formation. In total, these observations are consistent with a model in which STAT5 mediates specific FGF-induced angiogenic events in brain ECs.

Jak2 and Src are involved in FGF2- and FGF8b-induced activation of STAT5

Cytokine and growth hormone induced STAT activation is regulated by two pathways, one involving Jak family members and the other p60Src (34,35). To explore the role of Jak and Src in FGF-induced STAT activation, we tested whether pharmacologic inhibitors of these signaling molecules disrupt FGF-induced STAT activation. Both the Jak2 inhibitor, AG490, and the Src inhibitor, PP2, significantly diminishes STAT5 tyrosine phosphorylation (Fig. 6A,B). Conversely, the inactive forms of both PP2 (PP3) and AG490 (AG9) fails to show an inhibitory activity. FGF2-and FGF8b-induced STAT5 translocation to the nucleus is also inhibited by PP2 treatment (Fig. S2 and S3). The involvement of Jak2 in FGF signaling is further supported by the observation that FGF2 or FGF8b-dependent STAT5 activation is blocked by a dominant negative Jak2 (Jak2 K→E mutant) (Fig. S4). These results are consistent with Jak2 and Src acting upstream of FGF-induced STAT5 activation and are in keeping with the previously published observation that FGF2-induced STAT3 activation in HUVEC is associated with Jak2 and Src (16). Conversely, inhibition of Src by PP2 does not block the activation of ERK1/2 (Fig. 6B), indicating that distinct signaling pathways underlie FGF-induced STAT5 and MAPK pathway activation in mouse ECs. The Jak2 inhibitor AG490 reduces ERK1/2 phosphorylation, suggesting crosstalk between Jak2 and the MAPK pathway.

Src and Jak2 inhibitors block FGF2 and FGF8b-induced tube formation

The effect of Src and Jak2 inhibition on EC tube formation was examined to further explore the role of these tyrosine kinases in STAT5 signaling. FGF2- and FGF8b-induced tube formation is attenuated by treatment with either the Jak2 inhibitor, AG490 (Fig. 6C), or the Src inhibitor, PP2 (Fig. 6D). As expected, STAT5A-DN abrogates tube formation in the presence of either FGF2 or FGF8b. Expression of STAT5A-CA partially restores tube formation in the presence of PP2 or AG490. These results are consistent with Src and Jak2 signaling upstream of STAT5 although we cannot rule out that other Src and Jak2 dependent factors are also required for optimal EC morphogenesis.

Discussion

FGF family members are among the most potent angiogenesis inducers and actively participate in tumor angiogenesis. *In vitro*, both FGF2 and FGF8b stimulate EC proliferation, migration, invasion and tube formation. We show here that both FGFs stimulate STAT transcription factors, in particular STAT5. Importantly, we report the novel finding that FGF-induced STAT5 activation is necessary and sufficient for brain EC migration, invasion and tube formation, all of which are critical components of the angiogenic cascade. Conversely, STAT5 activation is dispensible for FGF-induced EC mitogenesis.

A considerable wealth of information has accumulated on signaling events downstream of the FGFR. Most attention has been directed toward the classical ras-raf-MEK-MAPK pathway [reviewed in (10,36)]. This signaling cascade appears to be primarily responsible for the regulation of cell proliferation. The PI3K-Akt pathway has been linked to FGF induced cell survival although Akt does not appear to be involved in FGF signaling in our cell model (9, 12,37). In agreement with our findings, a limited number of reports support a role for members of the STAT family in FGF signaling. For example, a constitutively active mutant FGFR3, which is responsible for thanatophoric dysplasia type II dwarfism, specifically activates STAT1, resulting in chondrocyte growth arrest (15). The FGFR-STAT1 axis also negatively regulates bone growth pre- and post-natally under physiological conditions (38,39). Deo et al. (16) observed STAT3 phosphorylation in response to FGF2 in human umbilical vein ECs,

which required platelet activating factor. The biologic consequence of STAT3 activation in this cell type was not further examined.

The multiplicity of the intracellular signaling pathways downstream of FGFR raises questions about their regulation and biologic purpose. It is conceivable that different FGFRs preferentially activate distinct signaling pathways (e.g. MAPK, Akt, STATs, or individual STAT family members). This hypothesis appears plausible as ECs isolated from diverse organ sites express different combinations of FGFRs (unpublished observation) and show distinct patterns of STAT activation. In bone ECs, FGF2 primarily stimulates STAT3, whereas FGF8b activates STAT5. Since FGF2 and FGF8b preferentially bind to and activate different FGFRs, this observation supports a model of FGFR-specific STAT activation. An attractive physiologic role for a network of divergent FGF signaling pathways might be that it generates numerous opportunities for crosstalk and integration with other signaling systems. For example, EGFR-mediated activation of ERK1/2 can diminish FGFR signaling via a negative feedback loop involving FRS2 (40). Interleukin-3 induced EC proliferation and migration is dependent on STAT5, which provides a mechanism for this cytokine (and probably other factors) to modulate FGF-mediated angiogenesis (41).

STAT proteins are activated by tyrosine phosphorylation through members of the Janus or Src kinase families (30). A direct activation by receptor tyrosine kinases has also been proposed (42). Our data point toward FGFR-induced STAT activation via Jak2 and Src intermediaries. The involvement of Jak2 downstream of a receptor tyrosine kinase indicates an unorthodox transduction mechanism for which there is some precedent. Dudley and co-workers described VEGF-induced STAT5 stimulation that required Jak2 activity (43). A role for Src family kinases in FGFR signaling has been described more frequently (20,21,44–46). Similar to our findings in ECs, Maciag's group (20) attributed FGF1-induced fibroblast migration to Src activation, whereas mitogenesis was associated with the ERK1/2 pathway. Claesson-Welsh's group (45) observed that Src inhibition abolishes FGF2-induced EC tube formation, consistent with the FGFR-Src-STAT5 signal cascade proposed here.

Our central observation is that STAT5 is required for FGF2 and FGF8b induced assembly of brain ECs into vascular tubes. This raises the question whether other pro-angiogenic factors can activate STATs, thus elevating STATs to the rank of general regulators of vascular endothelial morphogenesis. Indeed, the potent angiogenic stimulator VEGF induces tyrosine phosphorylation of several STAT family members, including STAT1, 3, 5 and 6 (43,47,48). Yahata and colleagues (48) found that VEGF-mediated STAT3 activation is essential for migration and tube formation in human dermal microvascular ECs. Consistent with the concept of EC heterogeneity, different STAT family members may be responsible for regulating the differentiation of ECs in different organ sites. Alternatively, both STAT3 and STAT5 may be required. The central role of STAT transcription factors in angiogenesis is further supported by the observation that the angiopoietin receptor, Tie-2, can activate STAT1, 3 and 5 (49). Interestingly, activated STAT3 was detected in tumor vessel ECs of gliomas, suggesting roles in tumor angiogenesis (17). Together, these studies point to an integration of several pro-angiogenic signaling pathways by STATs to orchestrate EC migration and organization into vascular channels.

The critical position of STAT family members in multiple pro-angiogenic signaling pathways renders them attractive targets for anti-angiogenic therapeutic approaches. Naturally, the involvement of STATs in cytokine signaling and their role in regulating the immune system and hematopoiesis may require very selective inhibition and/or targeted delivery of therapeutic agents. However, a recent preclinical study using a transcription factor decoy approach targeting STAT3 provided promising preliminary support for such a treatment strategy (50).

Additional work is needed to better define the FGFR-STAT signaling pathway and evaluate STATs as therapeutic targets.

Acknowledgements

This work was supported by NIH RO1 NS048921-01.

We thank Korise Rasmusson for help with the manuscript and Tom Pier for expert technical assistance with immunohistochemical staining.

References

1. Carmeliet P, Jain RK. Angiogenesis in cancer and other diseases. Nature 2000;407:249–257. [PubMed: 11001068]
2. Folkman J. Role of angiogenesis in tumor growth and metastasis. Semin Oncol 2002;29:15–18. [PubMed: 12516034]
3. Rong Y, Durden DL, Van Meir EG, Brat DJ. 'Pseudopalisading' necrosis in glioblastoma: a familiar morphologic feature that links vascular pathology, hypoxia, and angiogenesis. J Neuropathol Exp Neurol 2006;65:529–539. [PubMed: 16783163]
4. Slavin J. Fibroblast growth factors: at the heart of angiogenesis. Cell Biol Int 1995;19:431–444. [PubMed: 7543787]
5. Ornitz DM. FGFs, heparan sulfate and FGFRs: complex interactions essential for development. Bioessays 2000;22:108–112. [PubMed: 10655030]
6. Ornitz DM, Xu J, Colvin JS, et al. Receptor specificity of the fibroblast growth factor family. J Biol Chem 1996;271:15292–15297. [PubMed: 8663044]
7. Folkman J, Klagsbrun M, Sasse J, Wadzinski M, Ingber D, Vlodavsky I. A heparin-binding angiogenic protein--basic fibroblast growth factor--is stored within basement membrane. Am J Pathol 1988;130:393–400. [PubMed: 3277442]
8. Mattila MM, Ruohola JK, Valve EM, Tasanen MJ, Seppanen JA, Harkonen PL. FGF-8b increases angiogenic capacity and tumor growth of androgen-regulated S115 breast cancer cells. Oncogene 2001;20:2791–2804. [PubMed: 11420691]
9. Eswarakumar VP, Lax I, Schlessinger J. Cellular signaling by fibroblast growth factor receptors. Cytokine Growth Factor Rev 2005;16:139–149. [PubMed: 15863030]
10. Schlessinger J. Common and distinct elements in cellular signaling via EGF and FGF receptors. Science 2004;306:1506–1507. [PubMed: 15567848]
11. Kouhara H, Hadari YR, Spivak-Kroizman T, et al. A lipid-anchored Grb2-binding protein that links FGF-receptor activation to the Ras/MAPK signaling pathway. Cell 1997;89:693–702. [PubMed: 9182757]
12. Ong SH, Hadari YR, Gotoh N, Guy GR, Schlessinger J, Lax I. Stimulation of phosphatidylinositol 3-kinase by fibroblast growth factor receptors is mediated by coordinated recruitment of multiple docking proteins. Proc Natl Acad Sci U S A 2001;98:6074–6079. [PubMed: 11353842]
13. Kisseleva T, Bhattacharya S, Braunstein J, Schindler CW. Signaling through the JAK/STAT pathway, recent advances and future challenges. Gene 2002;285:1–24. [PubMed: 12039028]
14. Megeney LA, Perry RL, LeCouter JE, Rudnicki MA. bFGF and LIF signaling activates STAT3 in proliferating myoblasts. Dev Genet 1996;19:139–145. [PubMed: 8900046]
15. Su WC, Kitagawa M, Xue N, et al. Activation of Stat1 by mutant fibroblast growth-factor receptor in thanatophoric dysplasia type II dwarfism. Nature 1997;386:288–292. [PubMed: 9069288]
16. Deo DD, Axelrad TW, Robert EG, Marcheselli V, Bazan NG, Hunt JD. Phosphorylation of STAT-3 in response to basic fibroblast growth factor occurs through a mechanism involving platelet-activating factor, JAK-2, and Src in human umbilical vein endothelial cells. Evidence for a dual kinase mechanism. J Biol Chem 2002;277:21237–21245. [PubMed: 11940567]
17. Schaefer LK, Ren Z, Fuller GN, Schaefer TS. Constitutive activation of Stat3alpha in brain tumors: localization to tumor endothelial cells and activation by the endothelial tyrosine kinase receptor (VEGFR-2). Oncogene 2002;21:2058–2065. [PubMed: 11960378]

18. Cao X, Tay A, Guy GR, Tan YH. Activation and association of Stat3 with Src in v-Src-transformed cell lines. Mol Cell Biol 1996;16:1595–1603. [PubMed: 8657134]
19. Deo DD, Bazan NG, Hunt JD. Activation of platelet-activating factor receptor-coupled G alpha q leads to stimulation of Src and focal adhesion kinase via two separate pathways in human umbilical vein endothelial cells. J Biol Chem 2004;279:3497–3508. [PubMed: 14617636]
20. LaVallee TM, Prudovsky IA, McMahon GA, Hu X, Maciag T. Activation of the MAP kinase pathway by FGF-1 correlates with cell proliferation induction while activation of the Src pathway correlates with migration. J Cell Biol 1998;141:1647–1658. [PubMed: 9647656]
21. Zhan X, Plourde C, Hu X, Friesel R, Maciag T. Association of fibroblast growth factor receptor-1 with c-Src correlates with association between c-Src and cortactin. J Biol Chem 1994;269:20221–20224. [PubMed: 7519605]
22. Shuai K, Ziemiecki A, Wilks AF, et al. Polypeptide signalling to the nucleus through tyrosine phosphorylation of Jak and Stat proteins. Nature 1993;366:580–583. [PubMed: 7504784]
23. Langley RR, Ramirez KM, Tsan RZ, Van Arsdall M, Nilsson MB, Fidler IJ. Tissue-specific microvascular endothelial cell lines from H-2K(b)-tsA58 mice for studies of angiogenesis and metastasis. Cancer Res 2003;63:2971–2976. [PubMed: 12782605]
24. Si J, Collins SJ. IL-3-induced enhancement of retinoic acid receptor activity is mediated through Stat5, which physically associates with retinoic acid receptors in an IL-3-dependent manner. Blood 2002;100:4401–4409. [PubMed: 12393611]
25. Wang D, Stravopodis D, Teglund S, Kitazawa J, Ihle JN. Naturally occurring dominant negative variants of Stat5. Mol Cell Biol 1996;16:6141–6148. [PubMed: 8887644]
26. Hawker JR Jr. Chemiluminescence-based BrdU ELISA to measure DNA synthesis. J Immunol Methods 2003;274:77–82. [PubMed: 12609534]
27. Blair RJ, Meng H, Marchese MJ, et al. Human mast cells stimulate vascular tube formation. Tryptase is a novel, potent angiogenic factor. J Clin Invest 1997;99:2691–2700. [PubMed: 9169499]
28. Su G, Meyer K, Nandini CD, Qiao D, Salamat S, Friedl A. Glypican-1 is frequently overexpressed in human gliomas and enhances FGF-2 signaling in glioma cells. Am J Pathol 2006;168:2014–2026. [PubMed: 16723715]
29. Cao H, Dronadula N, Rizvi F, et al. Novel role for STAT-5B in the regulation of Hsp27-FGF-2 axis facilitating thrombin-induced vascular smooth muscle cell growth and motility. Circ Res 2006;98:913–922. [PubMed: 16527988]
30. Reich NC, Liu L. Tracking STAT nuclear traffic. Nat Rev Immunol 2006;6:602–612. [PubMed: 16868551]
31. Akhtar N, Dickerson EB, Auerbach R. The sponge/Matrigel angiogenesis assay. Angiogenesis 2002;5:75–80. [PubMed: 12549862]
32. Onishi M, Nosaka T, Misawa K, et al. Identification and characterization of a constitutively active STAT5 mutant that promotes cell proliferation. Mol Cell Biol 1998;18:3871–3879. [PubMed: 9632771]
33. Auerbach R, Lewis R, Shinners B, Kubai L, Akhtar N. Angiogenesis assays: a critical overview. Clin Chem 2003;49:32–40. [PubMed: 12507958]
34. Rane SG, Reddy EP. STATs and Src kinases in hematopoiesis. Oncogene 2002;21:3334–3358. [PubMed: 12032773]
35. Silva CM. Role of STATs as downstream signal transducers in Src family kinase-mediated tumorigenesis. Oncogene 2004;23:8017–8023. [PubMed: 15489919]
36. Eswarakumar VP, Ozcan F, Lew ED, et al. Attenuation of signaling pathways stimulated by pathologically activated FGF-receptor 2 mutants prevents craniosynostosis. Proc Natl Acad Sci U S A 2006;103:18603–18608. [PubMed: 17132737]
37. Zubilewicz A, Hecquet C, Jeanny JC, Soubrane G, Courtois Y, Mascarelli F. Two distinct signalling pathways are involved in FGF2-stimulated proliferation of choriocapillary endothelial cells: a comparative study with VEGF. Oncogene 2001;20:1403–1413. [PubMed: 11313884]
38. Sahni M, Ambrosetti DC, Mansukhani A, Gertner R, Levy D, Basilico C. FGF signaling inhibits chondrocyte proliferation and regulates bone development through the STAT-1 pathway. Genes Dev 1999;13:1361–1366. [PubMed: 10364154]

39. Xiao L, Naganawa T, Obugunde E, et al. Stat1 controls postnatal bone formation by regulating fibroblast growth factor signaling in osteoblasts. J Biol Chem 2004;279:27743–27752. [PubMed: 15073186]
40. Wu Y, Chen Z, Ullrich A. EGFR and FGFR signaling through FRS2 is subject to negative feedback control by ERK1/2. Biol Chem 2003;384:1215–1226. [PubMed: 12974390]
41. Dentelli P, Del Sorbo L, Rosso A, et al. Human IL-3 stimulates endothelial cell motility and promotes in vivo new vessel formation. J Immunol 1999;163:2151–2159. [PubMed: 10438956]
42. Clark DE, Williams CC, Duplessis TT, et al. ERBB4/HER4 potentiates STAT5A transcriptional activity by regulating novel STAT5A serine phosphorylation events. J Biol Chem 2005;280:24175–24180. [PubMed: 15863494]
43. Dudley AC, Thomas D, Best J, Jenkins A. A VEGF/JAK2/STAT5 axis may partially mediate endothelial cell tolerance to hypoxia. Biochem J 2005;390:427–436. [PubMed: 15918795]
44. Kanda S, Miyata Y, Kanetake H, Smithgall TE. Fibroblast growth factor-2 induces the activation of Src through Fes, which regulates focal adhesion disassembly. Exp Cell Res 2006;312:3015–3022. [PubMed: 16884713]
45. Klint P, Kanda S, Kloog Y, Claesson-Welsh L. Contribution of Src and Ras pathways in FGF-2 induced endothelial cell differentiation. Oncogene 1999;18:3354–3364. [PubMed: 10362356]
46. Zhang P, Greendorfer JS, Jiao J, Kelpke SC, Thompson JA. Alternatively spliced FGFR-1 isoforms differentially modulate endothelial cell activation of c-YES. Arch Biochem Biophys 2006;450:50–62. [PubMed: 16631103]
47. Bartoli M, Gu X, Tsai NT, et al. Vascular endothelial growth factor activates STAT proteins in aortic endothelial cells. J Biol Chem 2000;275:33189–33192. [PubMed: 10961983]
48. Yahata Y, Shirakata Y, Tokumaru S, et al. Nuclear translocation of phosphorylated STAT3 is essential for vascular endothelial growth factor-induced human dermal microvascular endothelial cell migration and tube formation. J Biol Chem 2003;278:40026–40031. [PubMed: 12874294]
49. Korpelainen EI, Karkkainen M, Gunji Y, Vikkula M, Alitalo K. Endothelial receptor tyrosine kinases activate the STAT signaling pathway: mutant Tie-2 causing venous malformations signals a distinct STAT activation response. Oncogene 1999;18:1–8. [PubMed: 9926914]
50. Xi S, Gooding WE, Grandis JR. In vivo antitumor efficacy of STAT3 blockade using a transcription factor decoy approach: implications for cancer therapy. Oncogene 2005;24:970–979. [PubMed: 15592503]

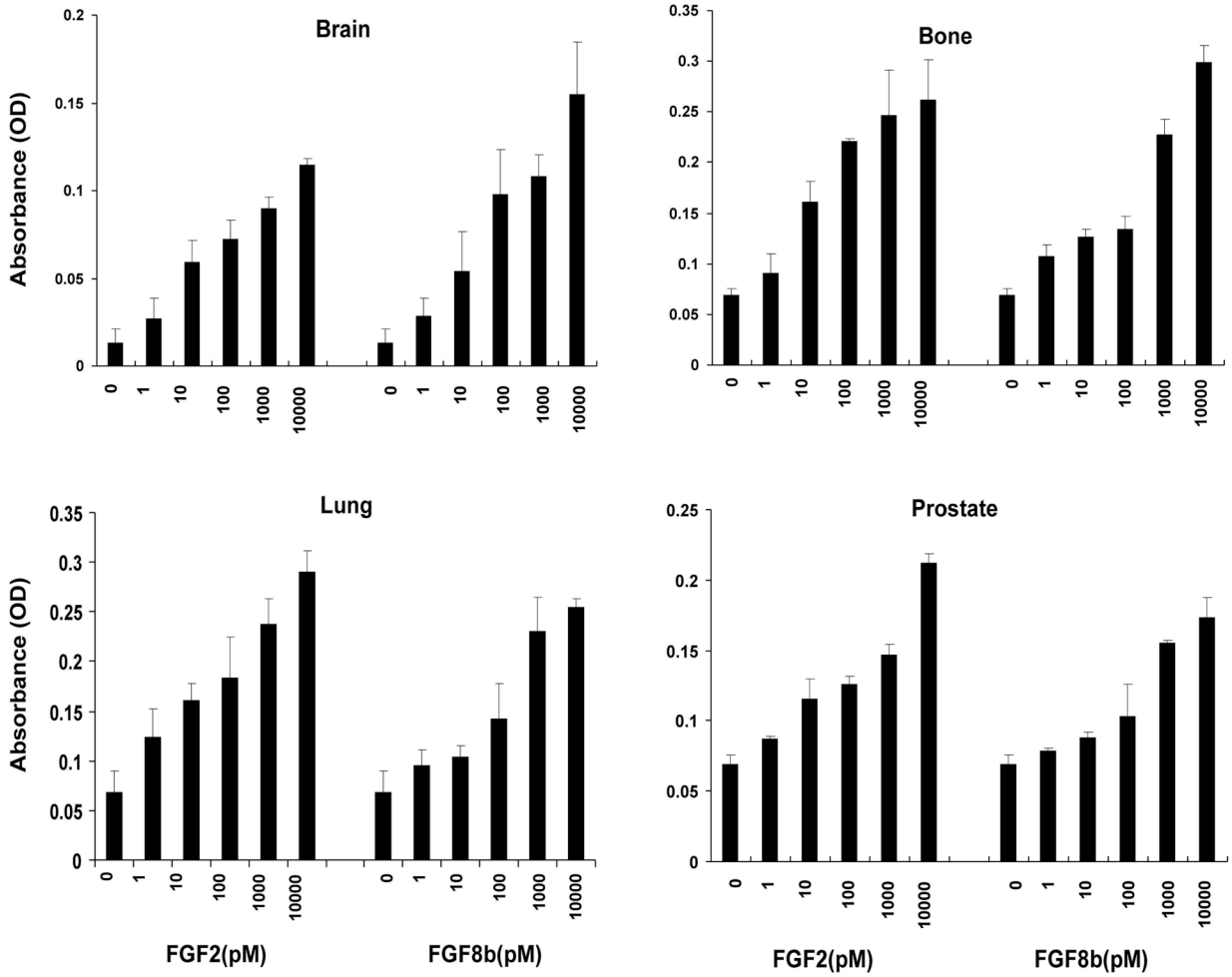

Fig. 1. FGF2 and FGF8b stimulate the proliferation of mouse microvascular ECs

Mouse ECs were starved for 24 hrs. and treated with the indicated concentrations of FGF2 or FGF8b in starvation medium for an additional 24 hrs. BrdU was added for the last 6 hrs and detected as described in Materials and Methods. The data are representative for three independent experiments. The error bars indicate standard deviation for triplicate samples in a single experiment.

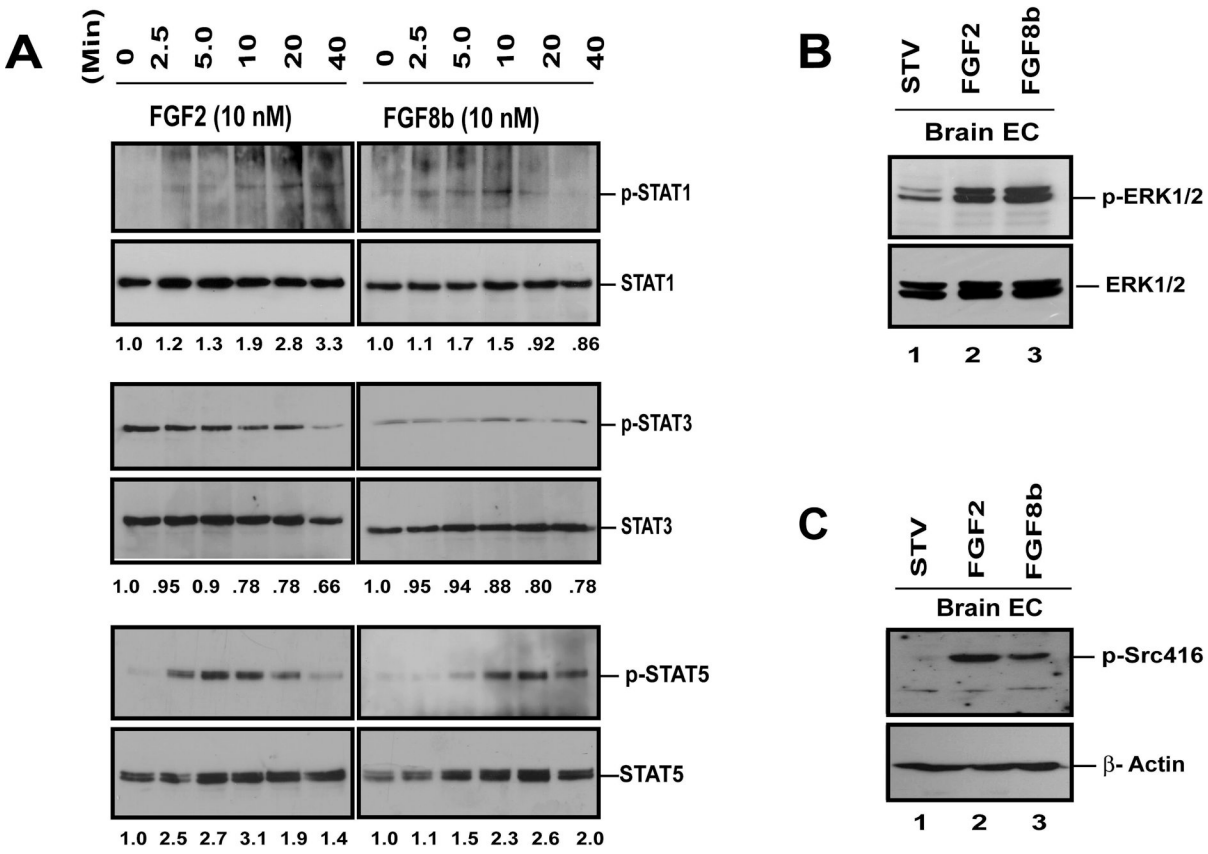

Fig. 2. FGF2 and FGF8b stimulate tyrosine phosphorylaton of STAT proteins in mouse brain microvascular ECs (BMVECs)

(A) Detection of FGF-induced tyrosine phosphorylation of STATs by Western blot. Cells at 90% confluence were starved for 24 hrs. and treated with 10 nM of FGF2 or FGF8b for 0, 2.5, 5, 10, 20 and 40 minutes as indicated. Cells were then lysed and immunoprecipited with different anti-STAT antibodies. Equal amounts of protein were separated with SDS-PAGE gels. The membranes were sequentially probed with antibodies to p-STATs and total STATs. Densitometry was performed with Kodak 1D 3.6 software and the results are listed below each band. (B) FGF2 and FGF8b-induced MAPK phosphorylation in BMVECs. (C) FGF2 and FGF8b-induced stimulation of Src phosphorylation in BMVECs. 50 μg of total protein of each sample were separated by SDS-PAGE and the membranes were probed with antibodies against p-Src. β-actin served as loading control.

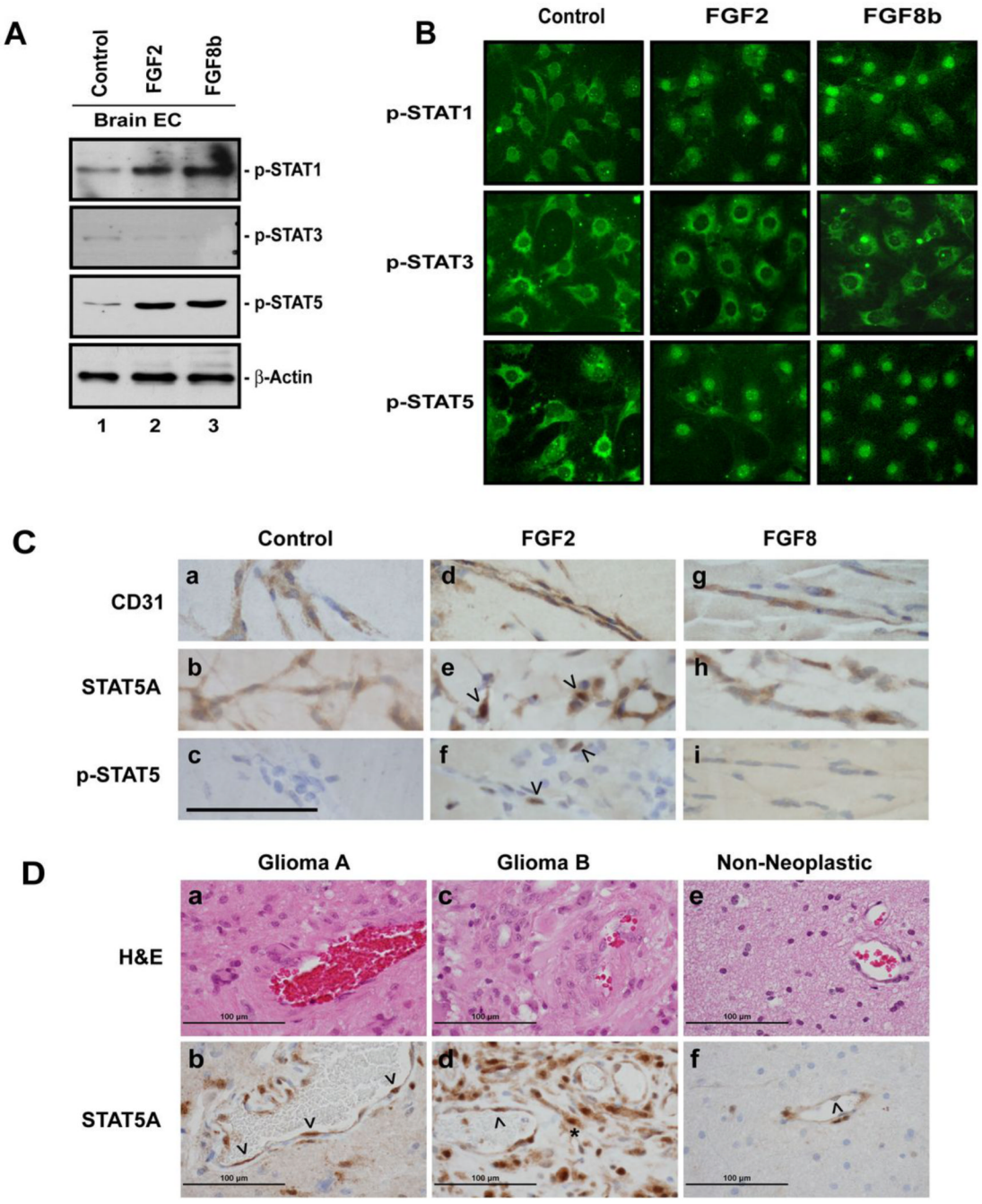

Fig. 3. FGF2 and FGF8b stimulate nuclear translocation of STAT proteins

(A) Analysis of phospho-STATs in nuclear fractions of FGF-stimulated BMVECs by Western blot. Cells at 90% confluence were starved for 24 hrs and stimulated with FGF2 or FGF8b (10 nM) for 30 minutes. 50 μg total protein of nuclear fractions were analyzed by SDS-PAGE to determine the amounts of p-STAT1, p-STAT3 and p-STAT5A. β-actin served as loading control. (B) Immunocytochemical detection of FGF2- and FGF8b-induced nuclear translocation of phospho-STATs in BMVECs. The cells were cultured to 50–75% confluency and then starved for 24 hrs. The cells were then stimulated with FGF2 or FGF8b (10 nM) for 10 minutes. After fixation with 4% paraformaldehyde and blocking, the cells were sequentially incubated with anti-p-STAT and fluorochrome-labeled secondary antibodies. Original

magnification x200. (C). STAT5 is activated during FGF2-induced angiogenesis *in vivo*. Matrigel with FGF2, FGF8b or without growth factor supplement (Control) was injected into Balb C mice. After 7 days, the matrigel plugs were excised and examined by immunohistochemical labeling with antibodies to the EC marker CD31, to STAT5A, and p-STAT5 as indicated. The arrowheads indicate EC nuclei; the scale bar represents 100 μm. Original magnification: 1,000x. (D). STAT5A localization in human glioma tissues: Paraffin sections from a tissue microarray containing human glioma tissues and non-neoplastic brain controls were hematoxylin-eosin stained (a, c, e) or labeled with an antibody to STAT5A (b, d, f). Bound antibody was visualized by immunoperoxidase (brown color signal). Two different glioma cases (a, b and c, d, respectively) and one nonneoplastic gliosis tissue (e,f) are shown. The arrowheads indicate vessel endothelial cell nuclei. The asterix indicates tumor cells with nuclear STAT localization. Original magnification: 600x.

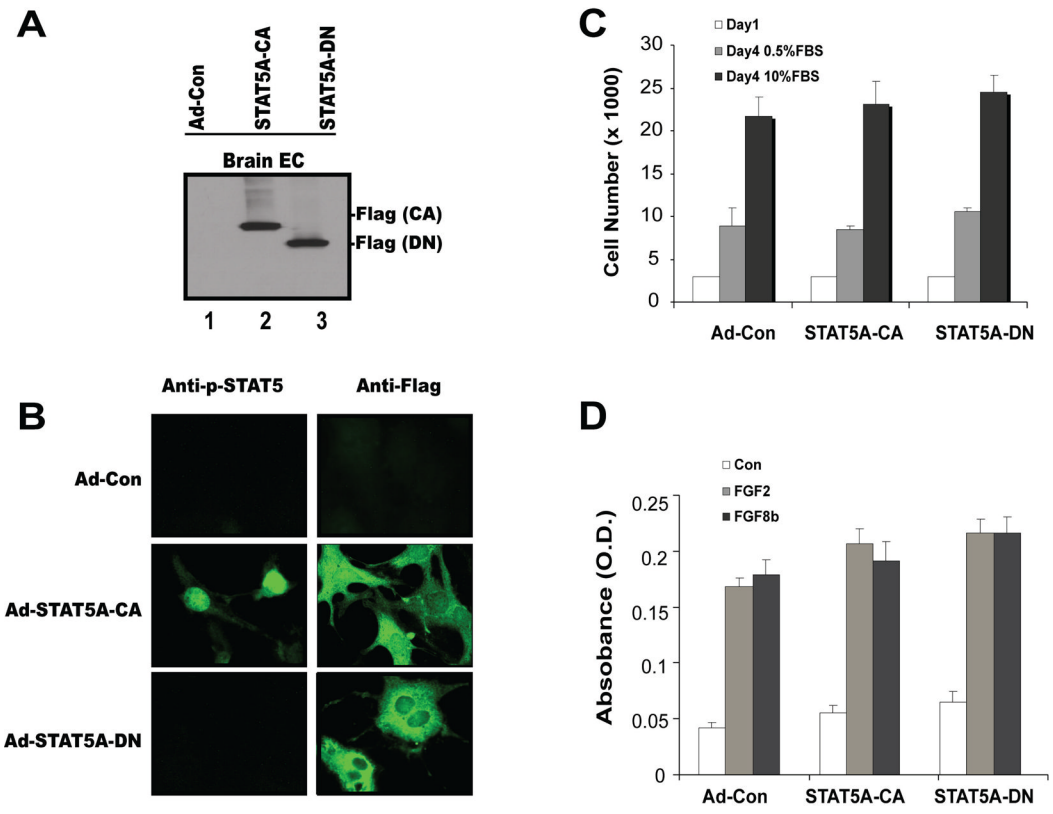

Fig. 4. STAT5 is not required for mitogenesis of BMVECs

(A) Expression of mutant STAT5A in brain ECs: BMVECs were transduced with mutant STAT5A adenovirus at 200 pfu/cell, lysed and processed for Western blotting. The membranes were probed with an anti-Flag antibody in order to detect ectopically expressed STAT5A. (B) Localization of mutant STAT5A in BMVECs: Cells were transduced with mutant STAT5A adenoviruses at 200 pfu/cell and labeled with antibodies to p-STAT5A and FLAG-tag (to detect exogenous STAT5A). (C) Forced expression of constitutively active STAT5A-CA or dominant-negative STAT5A-DN has no significant effect on cell growth compared with mock-infected cells. BMVECs transduced with the different adenoviruses were plated in triplicate wells in a 24-well plate in media containing either 0.5% or 10% serum. At the indicated time points, cells were harvested and viable cells were counted by trypan blue exclusion. Data represent the means ± SD of two experiments. (D) FGF2- and FGF8b-induced mitogenesis is independent of STAT5A. BMVEC mitogenesis in response to FGF2 and FGF8b was determined by BrdU assay in the presence and absence of STAT5A-CA and STAT5A-DN.

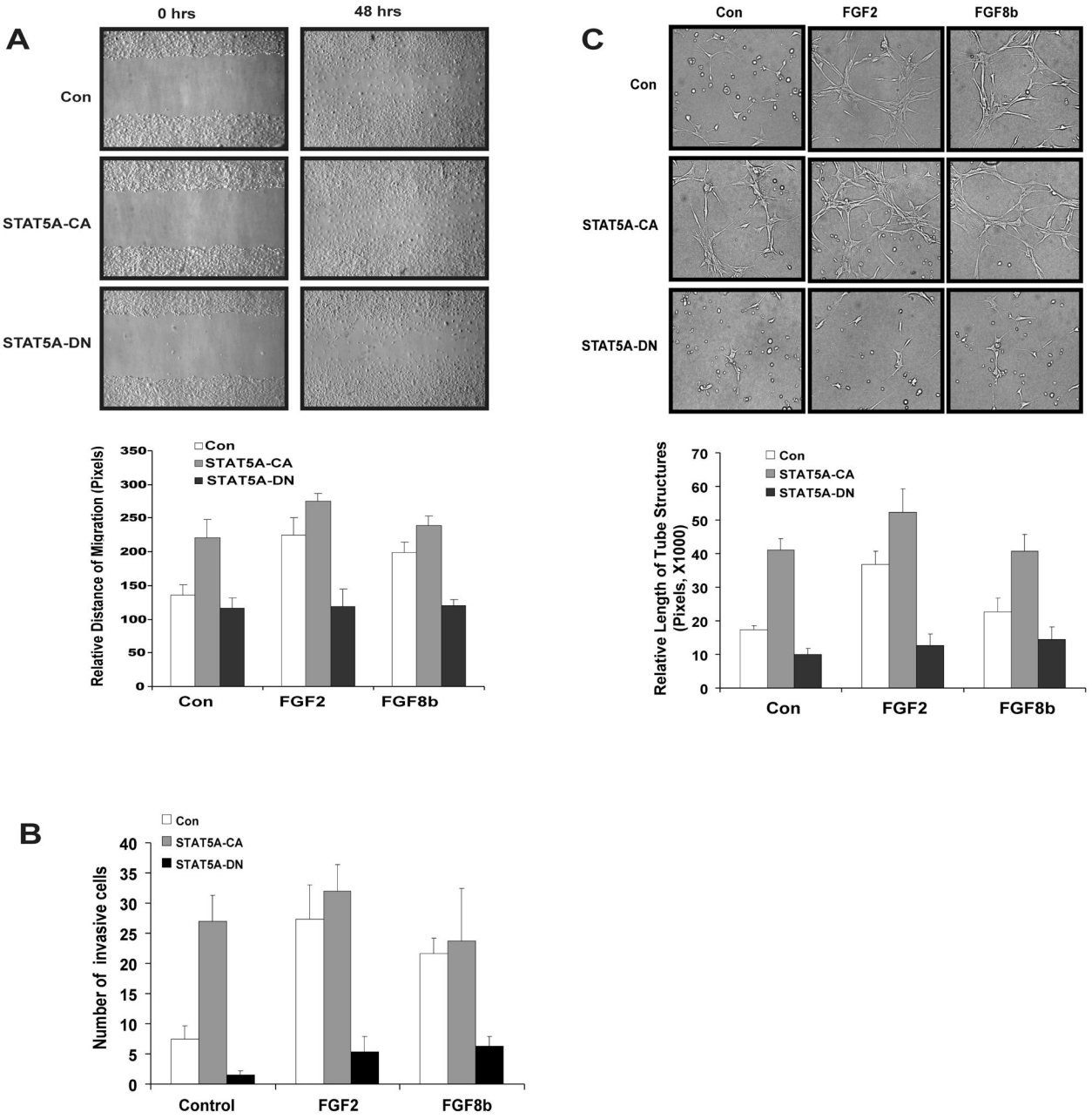

Fig. 5. STAT5 is necessary and sufficient for FGF2- and FGF8b-induced BMVEC migration and tube formation

(A) Dependence of BMVEC migration on STAT5A. BMVECs were infected with empty adenovirus (Con), adenovirus delivering constitutively active STAT5A-CA or dominant-negative STAT5A-DN at 100 pfu/cell. Cell monolayers at approximately 95% confluence after a 24 hr starvation period and 24 hr post-infection were wounded with a pipette tip (upper panels). Relative migration distance during the gap closure was measured with *ImageJ* (chart). STAT5A-CA largely bypassed the requirement for FGF2 or FGF8b ($p<0.01$). STAT5A-DN abolished FGF2- or FGF8b-induced migration ($p<0.01$). (B) Dependence of BMVEC invasion on STAT5A. BMVEC invasion was assayed using modified Matrigel invasion chambers. Cells (2×10^5) infected with control virus (Con) or mutant STAT5A delivering virus (STAT5A-CA and STAT5A-DN) were added to the upper chamber in the absence of FGFs. FGF-containing

medium (10 nM) was applied as a chemoattractant to the lower compartment of the chamber. Cells at the lower aspect of the membrane were counted after 48 hrs. Expression of STAT5A-CA stimulated invasion and bypassed the requirement for FGF2 or FGF8b ($p<0.01$). STAT5A-DN abolished FGF2- or FGF8b-induced invasion ($p<0.01$). (C) STAT5A is essential for EC tube formation in collagen gels. Mouse brain ECs expressing STAT5A-CA, STAT5A-DN and empty vector were tested for tube formation in collagen gels as detailed in Materials and Methods. EC tube formation was measured at 12 hrs. Photographs were taken with a phase-contrast microscope (upper panels) and relative tube length was measured with *ImageJ*, expressed as mean ± S.D. for three photographs (chart). STAT5A-CA stimulated tube formation and bypassed the requirement for FGF2 or FGF8b ($p<0.01$). STAT5A-DN abolished FGF2- or FGF8b-induced tube formation ($p<0.01$). Shown is one of three independent experiments.

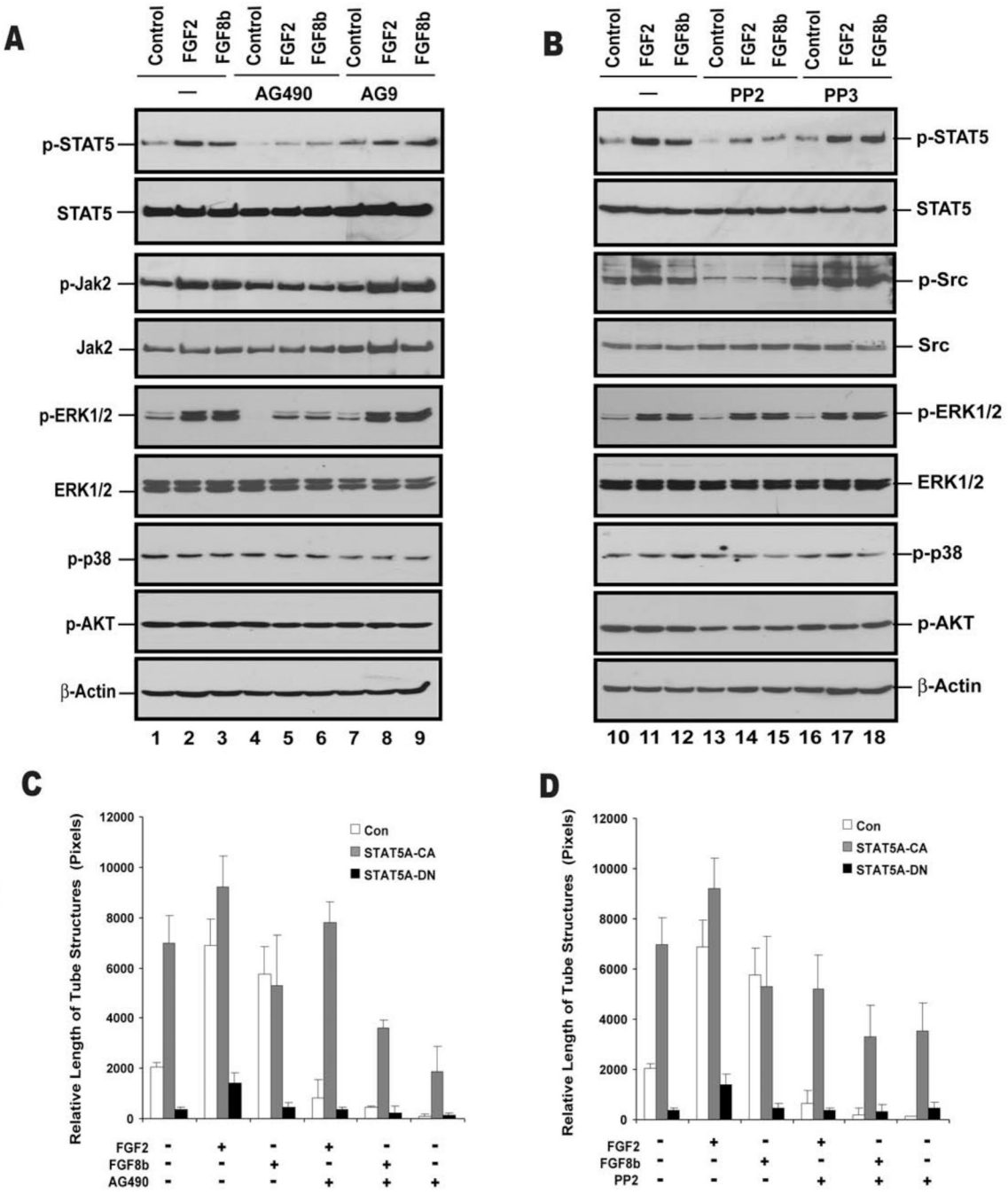

Fig. 6. Jak2 and Src activation are required for FGF2- and FGF8b-induced STAT5A phosphorylation and tube formation in BMVECs

Upper panel: Pharmacologic inhibitors of Jak2 (A) and Src (B) attenuate FGF2- and FGF8b-induced STAT5A phosphorylation in BMVECs. Cells at 90% confluence were starved and treated with the Jak2 inhibitor AG490 or the inactive analog AG9 (both at 30 μM for 24 hrs), and the Src inhibitor PP2 or the inactive analog PP3 (both at 10 μM for 16 hrs). FGF2 or FGF8b (10 nM) were then added for 20 min. Cell lysates were prepared, and 500 μg of total protein was used for immunoprecipitation with anti-STAT5A antibody. Phospho-STAT5A and total STAT5A were sequentially analyzed by Western blot. Levels of p-ERK1/2, ERK1/2, p-p38, p-AKT and β-actin were also assessed by Western blot as indicated. *Lower panel*: Jak2 and

Src activation are required for FGF2- and FGF8b-induced tube formation in BMVECs. Brain microvascular ECs were infected with Ad-Con, Ad-STAT5A-CA or Ad-STAT5A-DN at 100 pfu for 24 hrs, starved for 24 hrs and placed onto collagen gels (1.4 mg/ml) in the presence or absence of FGF2 or FGF8b (10 nM). The cells were treated with the Jak2 inhibitor AG490 at 30 μM (C) or the Src inhibitor PP2 at 10 μM (D). EC tube formation was measured at 12 hrs. Photographs were taken with a phase-contrast microscope and relative tube length was expressed as mean ± S.D. Both AG490 and PP2 inhibited FGF-induced tube formation and STAT5A-CA expression largely overcame this inhibition ($p<0.01$). Shown is one of two independent experiments.